

# All-*trans*-Retinaldehyde Contributes to Retinal Vascular Permeability in Ischemia Reperfusion

Alyssa Dreffs,<sup>1</sup> Cheng-Mao Lin,<sup>1</sup> Xuwen Liu,<sup>1</sup> Sumathi Shanmugam,<sup>1</sup> Steven F. Abcouwer,<sup>1</sup> Timothy S. Kern,<sup>2</sup> and David A. Antonetti<sup>1</sup>

<sup>1</sup>Department of Ophthalmology and Visual Sciences, University of Michigan Kellogg Eye Center, Ann Arbor, Michigan, United States

<sup>2</sup>Center for Translational Vision Research, Department of Ophthalmology, Gavin Herbert Eye Institute, School of Medicine, University of California-Irvine, Gillespie Neuroscience Research Facility, Irvine, California, United States

Correspondence: David A. Antonetti, Department of Ophthalmology and Visual Sciences, University of Michigan Kellogg Eye Center, 1000 Wall Street, Ann Arbor, MI 48105, USA; [dantonet@med.umich.edu](mailto:dantonet@med.umich.edu).

**Received:** January 7, 2020

**Accepted:** April 17, 2020

**Published:** June 3, 2020

Citation: Dreffs A, Lin C-M, Liu X, et al. All-*trans*-retinaldehyde contributes to retinal vascular permeability in ischemia reperfusion. *Invest Ophthalmol Vis Sci.* 2020;61(6):8. <https://doi.org/10.1167/iovs.61.6.8>

**PURPOSE.** Extracellular accumulation of all-*trans*-retinaldehyde (atRAL), a highly reactive visual cycle intermediate, is toxic to cells of the outer retina and contributes to retinal and macular degenerations. However, the contribution of atRAL to retinal capillary function has not been studied. We hypothesized that atRAL released from the outer retina can contribute to retinal vascular permeability. We, therefore, tested the contribution of atRAL to retinal ischemia-reperfusion (IR)-induced vascular permeability.

**METHODS.** IR was induced in mice by transient increase in intraocular pressure followed by natural reperfusion. The visual cycle was ablated in the *Lrat*<sup>-/-</sup> mice, reduced by dark adaptation or the use of the RPE65 inhibitor and atRAL scavenger emixustat. Accumulation of FITC-BSA was used to assess vascular permeability and DNA fragmentation quantified cell death after IR. Primary bovine retinal endothelial cell (BREC) culture was used to measure the direct effects of atRAL on endothelial permeability and cell death.

**RESULTS.** Inhibition of the visual cycle by *Lrat*<sup>-/-</sup>, dark adaptation, or with emixustat, all reduced approximately half of IR induced vascular permeability at 48 hours. An increase in BREC permeability with atRAL coincided with lactate dehydrogenase (LDH) release, a measure of cell death. Both permeability and toxicity were blocked by emixustat.

**CONCLUSIONS.** Outer retinal pathology may contribute to vascular permeability by release of atRAL, which can act directly on vascular endothelial cells to alter barrier properties and induce cell death. These studies may have implications for a variety of blinding eye diseases that include outer retinal damage and retinal vascular permeability.

**Keywords:** all-trans retinaldehyde, vascular permeability, ischemia reperfusion, blood retinal barrier

Diabetic retinopathy (DR) remains the leading cause of blindness in working age adults. Recent advances in therapy targeting vascular endothelial growth factor coupled with glucocorticoid treatment or laser photocoagulation provide effective treatment for many, but not all, patients that present with vascular dysfunction. Although much attention has focused on vascular abnormalities, there is intriguing clinical anecdotal evidence that loss of rod photoreceptors is protective against DR, a phenomenon that has been explained by the relative retinal hypoxia produced by the large oxygen demands of the rods. A survey of patients with diabetes with photoreceptor degeneration due to retinitis pigmentosa revealed less evidence of retinopathy, suggesting rods and cones contribute to the pathology of DR.<sup>1,2</sup>

Morphological studies of the outer retinal layer in animal models of diabetes have revealed varying results regarding loss of rod and cones or synaptic connectivity, but no definitive analysis has yet been provided (reviewed in Ref. 3). However, in animal models of diabetes, photoreceptors were identified as a major contributor of

oxidative stress because diabetic mice lacking photoreceptors due to opsin gene deletion or iodoacetic acid treatment exhibited dramatically reduced retinal superoxide production.<sup>4</sup> Further, spectral domain optical coherence tomography analyses revealed that the inner segment/outer segment (IS/OS), also called the inner segment ellipsoid band, and the external limiting membrane (ELM) were thinned in patients with DR, and that this outer retinal damage correlated with vision loss<sup>5</sup> and diabetic macular edema (DME).<sup>6,7</sup> Importantly, these outer retinal changes may persist after resolution of edema and loss of ELM integrity at the time of DME predicts poor visual acuity after resolution of edema.<sup>7</sup> A recent study found that patients with long-term diabetes but who are resistant to complications (Gold Medalists) possessed elevated intravitreal levels of retinal binding protein 3 (RBP3).<sup>8</sup> The RBP3, made by rods and cones, functions to transport retinols between cells as part of the visual cycle. Animal models of diabetes revealed diminished RBP3 content in vitreous and retina.<sup>8</sup> Furthermore, restoration of RBP3 levels, through injection of the protein, viral

gene delivery, or transgenic expression, ameliorated retinal vascular permeability, capillary dropout, and visual functional defects in diabetic rats and mice.<sup>8</sup>

The visual cycle regenerates 11-*cis*-retinal (11cRAL) for use as the chromophore of rod and cone visual pigments (reviewed in Refs. 9,10). Absorption of light by opsin-bound 11-cRAL leads to photoisomerization and release of the chromophore as all-*trans*-retinaldehyde (atRAL). The classic visual cycle describes conversion of free atRAL to all-*trans*-retinol (atROL) in rods by retinal dehydrogenase and transport to the retinal pigment epithelium (RPE) by RBP3. There, lecithin:retinol acyltransferase (LRAT) converts atROL to all-*trans*-retinyl ester (atRE) followed by isomerization to 11-*cis*-retinol (11cROL) catalyzed by the enzyme RPE 65kD protein (RPE65). Finally, the visual cycle is completed when 11cROL is converted to 11cRAL by dehydrogenase reaction and transported back to rods bound by RBP3. A similar intraretinal visual cycle utilizes Müller cells to produce 11cROL from atROL released by cones. Oxidation of 11cROL within cones then completes the regeneration of 11cRAL.

To prevent toxicity of the reactive aldehyde and promote efficiency of the visual cycle, the retinoid aldehyde intermediates are bound by cellular retinal binding proteins (CRALBPs) within cells and by RBP3 extracellularly. Using *Abca4*<sup>-/-</sup> *Rdh8*<sup>-/-</sup> mice, which are defective in both the transport of atRAL from the outer segment disk to the cytoplasmic surface and its dehydrogenation, respectively, Chen et al. demonstrated that abnormal accumulation of atRAL caused rod toxicity by nicotinamide adenine dinucleotide phosphate (NADPH) oxidase activation and reactive oxygen species (ROS) formation in a G-protein coupled receptor-dependent manner.<sup>11</sup> Toxicity due to abnormal accumulation of atRAL and its condensation products is associated with several degenerative retinal diseases, including Stargardt disease, retinitis pigmentosa (RP), and age-related macular degeneration (AMD).<sup>11</sup> AtRAL toxicity has been attributed to several mechanisms, including creation of oxidative and nitrosive stress,<sup>12</sup> ROS production leading to endoplasmic reticulum stress and mitochondrial dysfunction,<sup>13</sup> intracellular calcium elevation,<sup>14</sup> Bax-mediated apoptosis,<sup>15</sup> and NLRP3 inflammasome activation.<sup>16</sup>

Inhibitors of the visual cycle and atRAL scavengers have been developed for potential use as therapeutics. Given the evidence for outer retinal damage in diabetes, these same compounds are being explored in diabetic models. Animal studies have provided evidence that inhibition of RPE65 with retinylamine shows some protection from loss of visual acuity, capillary degeneration, and retinal vascular permeability induced by diabetes.<sup>17</sup> Emixustat (originally ACU-4429) is a primary-amine containing inhibitor of RPE65 retinoid isomerase activity.<sup>18</sup> The primary amine of emixustat also reacts with the aldehyde group of atRAL to form a Schiff base, thus effectively scavenging and detoxifying atRAL.<sup>19</sup>

In the current study, we wished to determine if atRAL toxicity can be extended to vascular cells and thus contribute to the retinal vascular permeability response following retinal injury. We explored the contribution of outer retinal atRAL toxicity to retinal vascular permeability using a mouse ischemia reperfusion (IR) model that we recently demonstrated to include a robust retinal vascular permeability response to injury.<sup>20</sup> DR contains an ischemic element that drives capillary leakage, but robust animal models of DR that recapitulate the human condition are not forthcoming. Although the IR model is not a model of human DR,

it is likely to model pathogenic elements of capillary leakage with corresponding clinical relevance. Here, we demonstrate that ablation of atRAL production in *Lrat* knockout mice, terminating the visual cycle by dark adaptation or inhibition of the visual cycle with emixustat, each significantly reduced, but did not ameliorate, IR-induced vascular permeability. In contrast, treatment with MB-002 to inhibit the visual cycle without sequestering atRAL did not inhibit the vascular permeability response. Further, we demonstrate that atRAL acts directly on endothelial cells in culture to induce cell damage and barrier permeability.

## MATERIALS AND METHODS

### Animal Care and Use

All animals were treated in accordance with the guidelines of the Institutional Animal Care and Use Committee of the University of Michigan College of Medicine and in compliance with the ARVO Statement for the Use of Animals in Ophthalmic and Visual Research. Animals were treated with emixustat or MB-002 24 hours before ischemia via intraperitoneal (IP) injection (8 mg/kg). In some cases, emixustat was injected 24 hours before ischemia and again 1 hour before ischemia. *Lrat*<sup>-/-</sup> mice were obtained from Jackson Laboratories (stock # 018866) and bred for studies. Dark adaptation was for 18 hours before ischemia, and for these animals, ischemia was performed under a dim red light after which they were returned to the dark room for 48 hours until harvest. The harvest also took place under a dim red light.

### Spectral Domain-Optical Coherence Tomography

In vivo images of retinal structure were obtained using a spectral domain-optical coherence tomography (SD-OCT) (Bioptigen, Durham, NC, USA). Rectangular volumes consisting of 1000 A-scans by 100 B-scans over a 1.4 × 1.4-mm area centered on the optic nerve head (ONH) were taken for visualization of retinal anatomy. Retinal thicknesses were measured at 350 μm from the ONH using the InVivoVue Diver Analysis software (Bioptigen). Measurements of total retinal thickness from the top of the retinal ganglion cell layer to the retinal pigment epithelium were obtained in nasal, temporal, superior, and inferior regions of the retina. The four measurements were averaged to generate an average total retinal thickness.

### Retinal Ischemia-Reperfusion Injury

Procedures were performed as previously described.<sup>20</sup> Briefly, animals were anesthetized, and ischemia was applied to the eyes by increasing the intraocular pressure (IOP) to cut off the blood supply from the retinal artery. Elevated IOP was maintained for 90 minutes by continuous injection of sterile saline through a needle inserted into the anterior chamber of the eye and connected to a hanging saline bag to provide 120 mm Hg of pressure. For the sham-treated group, contralateral eyes were treated by insertion of a needle into the anterior chamber of the eye through the cornea. IOPs of ischemic eyes were monitored using a microtonometer (TonoLab, Icare, Helsinki, Finland) and ranged from 75 to 100 mm Hg. Reperfusion occurred naturally after removal of the needle. Animals were harvested after 4 hours or 48 hours of reperfusion.

## Retinal Vascular Permeability

For measures of blood-retinal barrier (BRB) integrity using Sulfo-NHS Biotin deposition and cross linking, deeply anesthetized mice were injected in the femoral vein with Sulfo-NHS-Biotin that was allowed to circulate for 5 minutes, followed by flushing with PBS and perfusing with 2% paraformaldehyde (PFA) in PBS. Eyes were post fixed in PFA prior to retina dissection. Retinas were dissected and subjected to cryosection or whole mount staining and subsequent image analysis. Whole mount retinas or cross sections were incubated with rabbit anti-collagen intravenous (IV) antibody (Millipore) followed by Texas Red Streptavidin (Vector) and Alexa-Fluor 488 conjugated donkey anti-rabbit IgG (Jackson Immuno Research) secondary fluorescent antibody. Retina samples were imaged using Leica DM6000 fluorescent microscope and TCS SP5 confocal microscope (Leica, Wetzlar, Germany).

For FITC-BSA retinal accumulation as a measure of vascular permeability, procedures were performed as previously described.<sup>20</sup> Briefly, under anesthesia, animals received a femoral vein injection of FITC-BSA (200 mg/kg). After 2 hours, animals were re-anesthetized, blood samples were taken, and transcardially perfused with warm saline via the left ventricle for 2 minutes. Retinas were harvested and dried overnight; dry weights were used for data normalization. FITC-BSA was extracted from retinal tissues. Fluorescence of extracts and plasma samples was measured using a plate reader and compared to a standard curve. To obtain rates of FITC-BSA accumulation, retinal extract values were normalized to the plasma concentration, retinal dry weight, and dye circulation time.

## DNA Fragmentation

Procedures were performed as previously described.<sup>21</sup> Briefly, the presence of cytoplasmic nucleosomes formed by DNA cleavage was assayed using a Cell Death Detection ELISA kit (Roche, Indianapolis, IN, USA) according to the manufacturer's instructions. The results were expressed as optical density of light absorbance at 405 nm (with a 490 nm reference wavelength) and normalized to retinal wet weight.

## Bovine Retinal Endothelial Cell Culture

Primary BRECs were isolated and grown in culture as previously described.<sup>22,23</sup> Cell monolayer ion flux was measured by electrical resistance using an electrical cell-substrate impedance sensing (ECIS)-Z $\Theta$  system at 4000 Hz (Applied Biophysics, Troy, NY, USA). BRECs were seeded on 8-well 8W10E<sup>+</sup> ECIS plates containing gold electrodes. Cells were left to grow overnight, followed by media change to step-down media (1% serum and 100 nm hydrocortisone) for 48 hours. Cells were treated with atRAL (Sigma) (10  $\mu$ M), the resistance was recorded for 48 hours after the addition of atRAL at the indicated concentration. BRECs were seeded on 0.4  $\mu$ m pore transwell filters (Corning Costar, Acton, MA, USA) in MCDB media and switched to stepdown media 48 hours before the start of the experiment. The cells were treated with atRAL, emixustat or atRAL, and emixustat at the indicated concentration. Cell monolayer permeability to 70 kDa FITC-dextran (Sigma) was determined as previously described.<sup>23</sup>

## Lactate Dehydrogenase Release Assay

Cell cytotoxicity was assessed using the CytoTox 96 Cytotoxicity Assay (Promega Corporation, Madison, WI, USA) according to the manufacturer's protocol. Briefly, cells were incubated for 4 or 48 hours after the addition of atRAL or DMSO control at 37°C and the relative accumulated lactate dehydrogenase (LDH) activity in media measured and normalized to the maximum possible LDH release caused by complete cell lysis. To determine the maximum LDH that could be released, lysis solution was added to control wells 45 minutes prior to supernatant harvest. The assay was performed using 50  $\mu$ L supernatant from each well of the assay plate, this was combined with 50  $\mu$ L/well reconstituted substrate mix. Stop solution was added after a 30 minute incubation followed by reading the absorbance at 490 nm.

## Statistical Analysis

All studies were repeated in duplicate or triplicate and presented as an accumulation of multiple independent experiments. Statistical analysis was performed using Prism software (GraphPad, La Jolla, CA, USA) using one-way analysis of variance with Tukey's or Sidak's post hoc analysis for multiple conditions or by *t*-test with two conditions and a *P* < 0.05 was considered statistically significant. All data is expressed as mean  $\pm$  SEM with \* < 0.05, \*\* < 0.01, \*\*\* < 0.001, or \*\*\*\* < 0.0001.

## RESULTS

### Sulfo-NHS-Biotin Leak is Increased Following IR Injury

Previous studies have revealed that IR injury induces a rapid increase in permeability of the retina followed by inflammation in mice.<sup>20</sup> In rats, the IR-induced permeability has been shown to be dependent on vascular endothelial growth factor,<sup>21,24,25</sup> modeling aspects of vascular alterations in retinal eye diseases, such as DR and retinal vein occlusion. Here, sulfo-NHS-biotin accumulation and crosslinking was used to identify regions of increased permeability. Whole mount images of retinas after IR revealed extensive sulfo-NHS-biotin staining compared to very little deposition in the control samples (Fig. 1A). Cross sections of the retinas revealed that permeability to the sulfo-NHS-biotin occurred adjacent to blood vessels with high co-localization with Col IV-positive basement membranes around blood vessels (Fig. 1B). The sulfo-NHS-biotin deposition was observed in the inner retina near the vasculature with limited or no deposition in the outer retina.

### Genetic Inhibition of Visual Cycle Reduces Permeability and Cell Death Following IR Injury

In order to determine the contribution of the outer retinal visual cycle to IR-induced retinal vascular permeability, we tested the effect of IR injury on *Lrat*<sup>-/-</sup> mice that are defective in formation of all-*trans*-retinyl ester in the RPE, ultimately preventing formation of atRAL. Ischemia was induced in *Lrat*<sup>-/-</sup> mice and C57BL/6J age matched controls and permeability to FITC-BSA was measured at 48 hours after reperfusion by extracting and quantifying the deposited dye (Fig. 2A). In wildtype C57BL/6J controls, vascular permeability increased 5.8-fold (*P* < 0.0001, Sham versus IR) in IR reti-

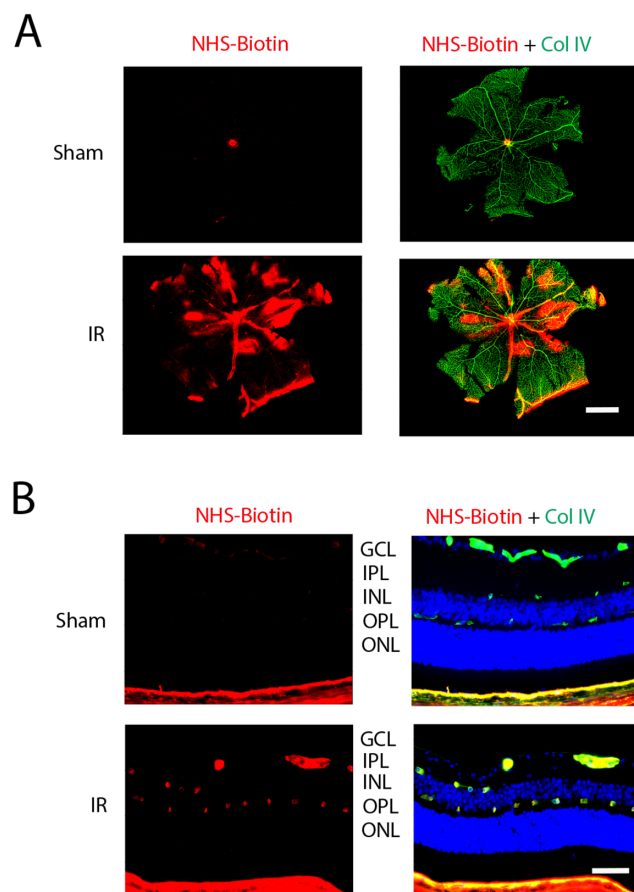


**FIGURE 1.** Retinal IR injury caused vascular permeability. Mice underwent IR injury and sulfo-NHS-biotin deposition and crosslinking was measured at 48 hours after reperfusion. (A) Whole mount retinas with full field view (scale bar, 1 mm) or (B) cross sections (scale bar, 50  $\mu$ m) were stained with sulfo-NHS-biotin (red) and with anti-Col IV antibody (green). The sulfo-NHS-biotin co-localized with Col-IV near inner retinal blood vessels. Example image of two retinas with identical results.

nas when compared to sham retinas as determined by FITC-BSA accumulation. Vascular permeability in *Lrat*<sup>-/-</sup> mice increased 3.7-fold ( $P < 0.01$ , *Lrat*<sup>-/-</sup>-Sham versus *Lrat*<sup>-/-</sup>-IR) 48 hours after ischemia. When comparing IR versus *Lrat*<sup>-/-</sup>-IR, there was an approximately 50% reduction in permeability in the *Lrat*<sup>-/-</sup>-IR compared to control IR ( $P < 0.05$ , IR versus *Lrat*<sup>-/-</sup>-IR,  $n \geq 13$ ). Thus, lack of a functioning visual cycle diminished the vascular leakage observed after IR injury.

To determine if vascular permeability caused retinal edema, the effects of IR injury on retinal thickness were determined using optical coherence tomography (OCT; Fig. 2B). IR induced a slight but significant 6.2% increase in retinal thickness in C57BL/6J mice at 48 hours. As expected, both sham and IR retinas in the *Lrat*<sup>-/-</sup> mice were significantly thinner than the retinas of C57BL/6J mice due to retinal degeneration, in contrast to control mice, retinas of *Lrat*<sup>-/-</sup> mice exhibited no increase in retinal thickness after IR. Thus, not only was vascular leakage attenuated, but apparent retinal edema after IR injury was prevented in *Lrat*<sup>-/-</sup> mice.

A DNA fragmentation assay was used to determine the effect of *Lrat* deficiency on retinal cell death at 48 hours after

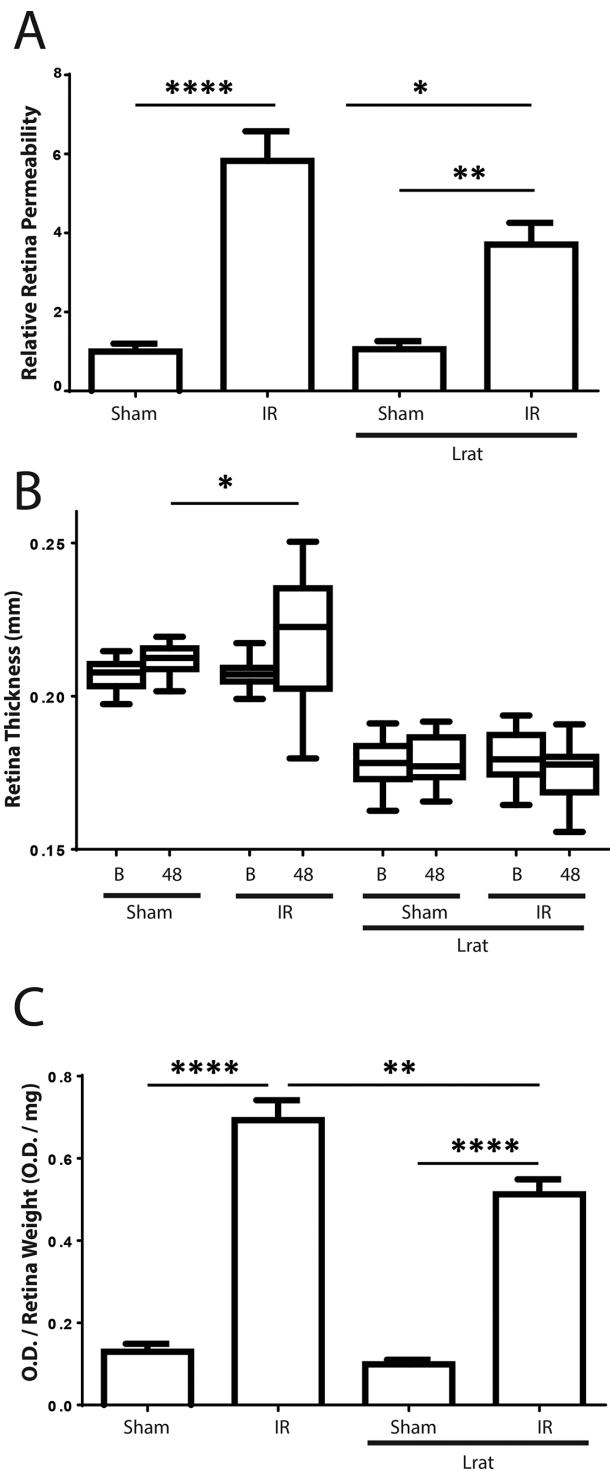


**FIGURE 2.** *Lrat*<sup>-/-</sup> reduces IR-induced retinal pathology. (A) *Lrat*<sup>-/-</sup> mice or age matched controls underwent IR injury and permeability to FITC-BSA was measured at 48 hours after reperfusion. *Lrat*<sup>-/-</sup> mice had significantly reduced permeability response, but permeability was still significantly increased in response to injury. Results are expressed relative to the vehicle-sham group with an  $n \geq 13$  for each group. (B) *Lrat*<sup>-/-</sup> mice were imaged by OCT before ischemia B and at 48 hours after reperfusion with an  $n \geq 13$ /group. Control animals reveal an increase in thickness indicative of edema caused by IR injury, a response that was absent in *Lrat*<sup>-/-</sup> mice. (C) *Lrat*<sup>-/-</sup> mice exhibit reduced DNA fragmentation after IR. At 48 hours after IR, *Lrat*<sup>-/-</sup> mice or age matched control animals were euthanized and retinas were harvested for DNA fragmentation ELISA assay, with  $n \geq 8$ /group. *Lrat*<sup>-/-</sup> mice demonstrated less cell death at 48 hours after IR compared to control IR animals.

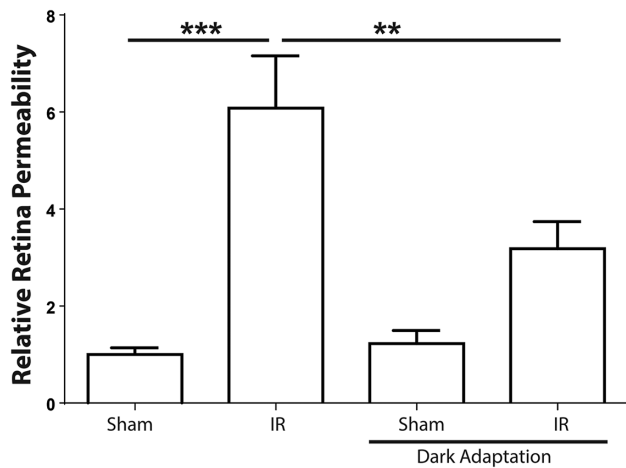


**FIGURE 3.** Dark adaptation reduces permeability 48 hours after IR injury. Mice were dark adapted for 18 hours prior to IR injury. For dark-adapted animals, the ischemia procedure was performed under dim red light and animals were returned to dark housing for 48 hours, until being harvested under dim red light. Light-adapted control mice were kept in normal dark/light cycle for the entire 72 hour period. Results are expressed relative to sham under normal light conditions with an  $n \geq 21$ /group. Dark adaptation significantly reduced IR induced permeability.

ischemia. Compared to sham control groups, IR-injured retinas of both control and *Lrat*<sup>-/-</sup> mice demonstrated greatly increased cell death; however, the increase in retinas of the *Lrat*<sup>-/-</sup> mice was 26% less than that caused by injury of the C57BL/6J retinas (Fig. 2C). Thus, *Lrat*<sup>-/-</sup> mice that lack the visual cycle and do not produce atRAL, exhibited less retinal cell death following IR injury.

### Dark Adaptation Blocks Permeability After IR Injury

To further explore the contribution of the visual cycle to retinal vascular permeability after IR injury, we used dark adaptation in C57BL/6J mice. The visual cycle and levels of retinoids are dramatically reduced by dark adaptation, with atRAL decreasing from 165 pmol/eye in light to 16 pmol/eye in the dark.<sup>26</sup> Mice were dark adapted for 18 hours, the IR procedure was carried out under dim red light, and the animals returned to a dark room after IR. This experimental group was compared to control animals that were maintained in the normal 12 hours light/12 hours dark cycle before and after IR and underwent ischemia in the light. Animals were processed at the same time to avoid confounding diurnal cycle effects. Vascular permeability was significantly increased by 6.1-fold ( $P < 0.0001$ ) in IR retinas 48 hours after ischemia when compared to sham retinas (Fig. 3). Strikingly, animals housed in the dark, prior to and following, ischemia, exhibited a significantly reduced permeability response of only 2.6-fold. Thus, similar to the effects of lacking the visual cycle in *Lrat*<sup>-/-</sup> mice, the permeability response to injury in dark adapted mice was again approximately half that of the control animals.

### Emixustat Treatment Abates Permeability After IR Injury

In order to further determine whether the visual cycle activity contributes to alterations in vascular permeability and

to help identify the mechanism of vascular dysfunction, we treated C57BL/6J mice with visual cycle inhibitors. Emixustat acts as both an inhibitor of RPE65 and as an atRAL scavenger via its primary amine.<sup>19</sup> Animals were treated via IP injection with a single dose of emixustat at 24 hours before ischemia and compared to control animals treated with vehicle injection. Vascular permeability was significantly increased by 2.6-fold in control animals 48 hours after IR ( $P < 0.0001$ , Fig. 4A). Similar to the effects seen in *Lrat*<sup>-/-</sup> and dark-adapted mice, treatment with emixustat significantly reduced the effect of IR on vascular permeability ( $P < 0.05$ ), with only a 1.9-fold increase in treated mice. Emixustat was previously shown to both inhibit RPE65, thus reducing the visual cycle, and to form a Schiff base between its primary amine and the aldehyde group of atRAL, thus act as a detoxifying scavenger.<sup>19</sup> MB-002 is a derivative of emixustat with an alcohol group substituted for the primary amine group. MB-002 exhibits the same ability to inhibit RPE65 activity in vivo, but without the ability to react with and sequester atRAL.<sup>19</sup> Treatment with an identical dosage of MB-002 had no effect on the vascular permeability caused by IR (see Fig. 4A), suggesting both chemical inhibition of the visual cycle and atRAL scavenging are necessary for inhibition of vascular leak after injury. Emixustat did not alter IR-induced retinal cell death at 48 hours after ischemia, as no difference in the increase of DNA fragmentation caused by IR injury was observed between emixustat-treated and control mice (Fig. 4B).

Because emixustat only induced a partial reduction in permeability after IR, we increased the injections of this drug to determine if this could further decrease vascular permeability after IR injury. Mice were treated with a first dose of emixustat at 24 hours before ischemia and a second dose 1 hour before ischemia. The results show that an additional dose of emixustat yielded similar inhibition of the permeability response as previously seen with a single dose given 24 hours before ischemia, with a reduction of approximately half of the IR induced permeability (Supplementary Fig. S1).

The effect of emixustat on atRAL production and scavenging was further substantiated using *Lrat*<sup>-/-</sup> mice. Because *Lrat*<sup>-/-</sup> mice fail to generate atRAL, we hypothesized that emixustat would have no further effect on the reduction of permeability observed in *Lrat*<sup>-/-</sup> mice. Figure 4C demonstrates that *Lrat*<sup>-/-</sup> animals treated with emixustat did not display a further attenuation of the permeability response compared to the untreated *Lrat*<sup>-/-</sup> animals, thus substantiating emixustat's effect on inhibition of visual cycle as the mechanism of action in reducing vascular permeability after IR injury.

Previous studies in rats have demonstrated that IR induces a rapid vascular endothelial growth factor-dependent increase in vascular permeability that is measurable within hours, long before increase in inflammatory factor expression.<sup>25</sup> Because emixustat is thought to act by preventing atRAL production and sequestering eventual atRAL released from damaged photoreceptors, we hypothesized that it would have no effect on the immediate vascular permeability response to IR injury. Emixustat was, therefore, injected 24 hours before IR and permeability was assessed at 4 hours after ischemia. Unlike at 48 hours after IR injury, emixustat was not effective at blocking vascular permeability at this early time point. Vascular permeability was significantly increased in both control (3.4-fold) and emixustat treated (3.3-fold) animals, with no significant difference between these groups (Fig. 4D). These data are consis-

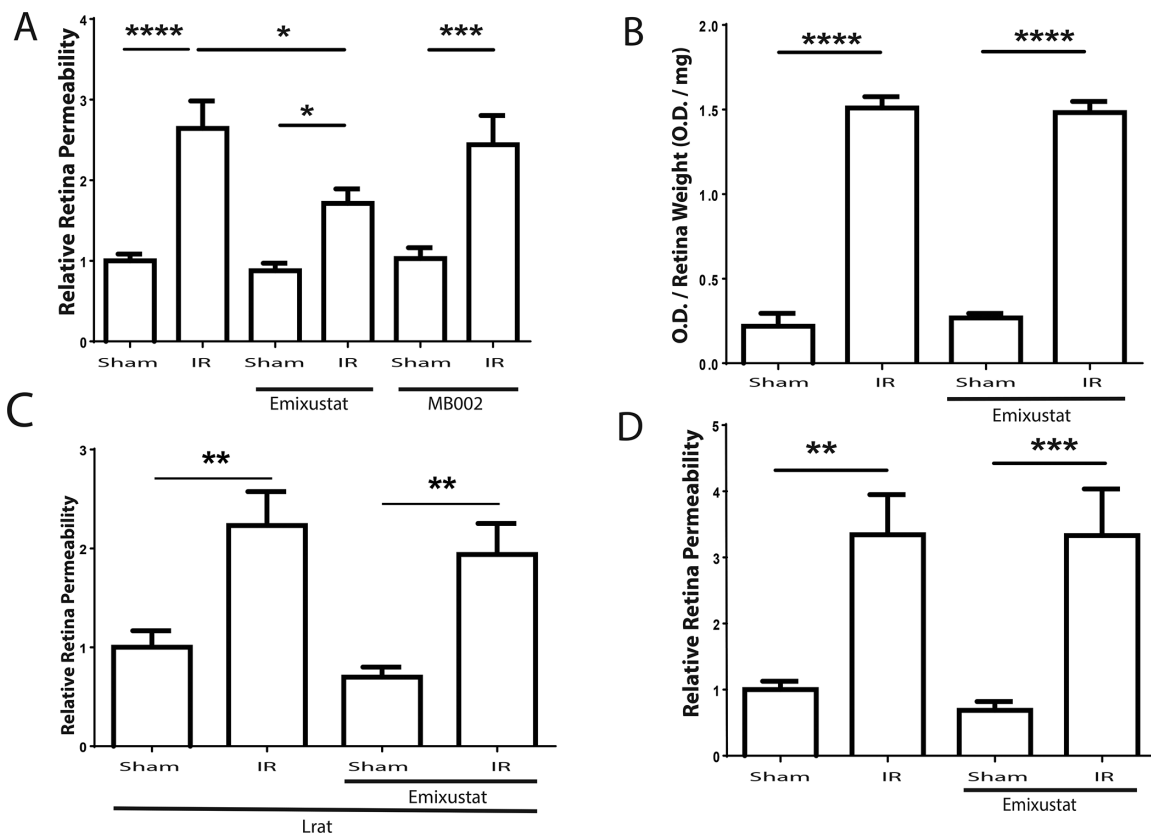


**FIGURE 4.** Inhibition of RPE65 with emixustat reduces permeability 48 hours after IR injury. (A) C57BL/6J mice were treated with emixustat or MB002 by IP injection at 24 hours before ischemia. At 48 hours after IR, animals were evaluated for vascular permeability of FITC-BSA. Results are expressed relative to the vehicle-sham group, where  $n \geq 17$ /group. Emixustat significantly reduced permeability of FITC-BSA after IR compared to vehicle-treated control, but MB-002 did not have a significant effect. (B) Emixustat does not affect IR-induced cell death. C57BL/6J mice were treated with emixustat 24 hours before ischemia. At 48 hours after IR, animals were euthanized and retinas were harvested for DNA fragmentation assay with an  $n \geq 7$ . (C) Emixustat does not have any additive effect on permeability in  $Lrat^{-/-}$  mice.  $Lrat^{-/-}$  mice were treated with emixustat 24 hours before ischemia and at 48 hours after IR animals were tested for FITC-BSA permeability and compared to  $Lrat^{-/-}$  mice without emixustat. Results are expressed relative to the  $Lrat^{-/-}$  mice sham-group, with an  $n \geq 13$ /group. (D) Emixustat does not affect early permeability after IR. C57BL/6J mice were treated with emixustat 24 hours before IR injury and permeability to FITC-BSA was measured beginning at 4 hours after reperfusion. Results are expressed relative to the vehicle-sham group, with  $n \geq 13$ /group.

tent with the hypothesis that ischemia induced outer retinal damage leading to release and extracellular accumulation of atRAL that contributed to retinal vascular permeability, perhaps by directly acting upon vascular cells.

### All-trans Retinal Induces Permeability in Endothelial Cell Culture

In order to directly assess the effect of atRAL on endothelial barrier properties and viability, primary endothelial cell culture was used. Barrier properties of BREC treated with atRAL were studied using real-time measures of *trans*-endothelial electrical resistance (TEER), a measure of ion permeability across the monolayer, using the ECIS Z-theta system with 4000 Hz cycling. Treatment of BREC with 10  $\mu$ M atRAL caused a 25% decrease in TEER by 4 hours after treatment (Fig. 5A). This initial effect resolved over the course of the next 12 hours, followed by secondary decrease in TEER starting at 32 hours and reaching approximately 20% at 48 hours. Using BREC grown on 0.4  $\mu$ m pore-containing

Transwell filters, the effects of atRAL treatment on endothelial permeability to a 70 kDa FITC-dextran tracer was also measured over a 4 hour time course. It was found that both 8 and 10  $\mu$ M atRAL caused a dramatic increase in solute permeability when compared to control cells, although neither 4 or 6  $\mu$ M atRAL caused any change in permeability (Fig. 5B). Permeability was also assessed 48 hours after the addition of atRAL and no difference was seen between control and 10  $\mu$ M atRAL treated cells (Supplementary Figure S2) indicating the effect of atRAL is transient.

As expected, co-treating cells with emixustat to sequester and detoxify the atRAL was able to block the effect of atRAL on BREC permeability. Cells were treated with emixustat alone, atRAL alone, or emixustat plus atRAL and permeability measurements began 2.5 hours after the addition of the compounds (Fig. 5C). Treatment with 16  $\mu$ M of emixustat alone had no effect on 70 kDa dextran permeability. Treatment with 8  $\mu$ M atRAL alone again increased permeability, although inclusion of either 16 or 8  $\mu$ M emixustat along with 8  $\mu$ M atRAL completely prevented the atRAL-induced permeability. These studies demonstrate that atRAL directly

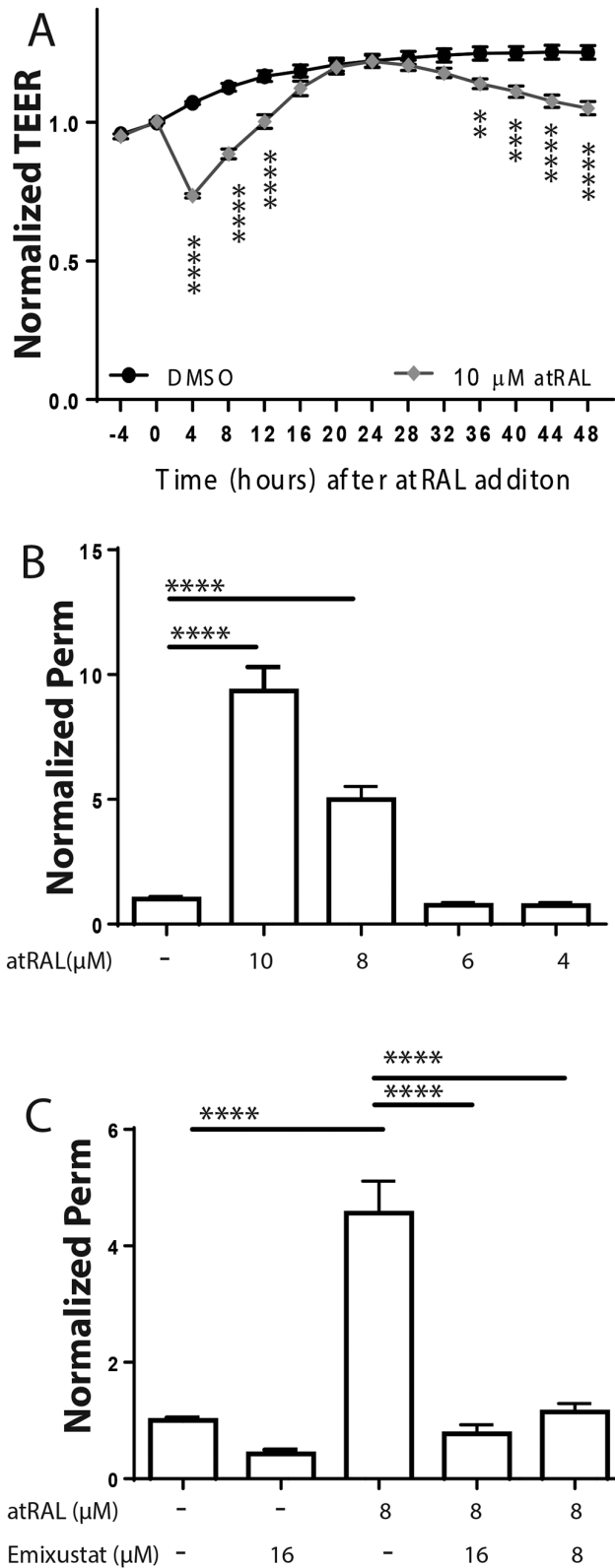


**FIGURE 5.** AtRAL induces permeability in BREC cell culture. (A) BREC cells were plated on 8-well ECIS chambers for measure of TEER with an alternating current frequency of 4000 Hz. Confluent cell cultures were switched to stepdown media 48 hours prior to being treated with atRAL at the indicated final concentrations and electrical resistance was recorded for 48 hours following atRAL addition. Data ( $n \geq 8$ /group) are presented with (asterisk) indicating time points with significant differences compared to DMSO-treated

induces endothelial permeability and the scavenger activity of emixustat can prevent this effect on endothelial barrier properties.

**All-trans Retinal Causes Endothelial Cell Death**

The effects of atRAL concentration on the endothelial cell death were assessed by measuring the amount of LDH released into the media at 4 hours after atRAL addition to the cultures. Significant amounts of LDH were released when atRAL was added at concentrations greater than or equal to 6 μM, with LDH release reaching approximately 50% that caused by total cell lysis at a concentration of 30 μM atRAL (Fig. 6A). The addition of 8 μM emixustat at the same time as atRAL was able to completely prevent the release of LDH into the media (Fig. 6B). LDH release was also tested at 48 hours after the addition of atRAL. According to the manufacturer of the LDH assay, LDH has an estimated half-life of 9 hours in the media (Promega). At 48 hours after atRAL addition, the release of LDH was not different when compared to control (see Supplementary Fig. S2).

**DISCUSSION**

The current study provides strong evidence that atRAL released from damaged photoreceptors contributes to capillary permeability after retinal injury by directly causing toxicity to endothelial cells. Using a mouse IR injury model that exhibits sustained retinal vascular permeability, we reveal that preventing the visual cycle and blocking atRAL production by genetic ablation of *Lrat* or dark adaptation, or slowing the visual cycle by inhibiting RPE65 with emixustat treatment, ameliorates approximately half of the IR-induced vascular permeability to FITC labeled albumin at 48 hours after ischemia. Further, emixustat treatment had no further effect on the permeability response in the *Lrat*<sup>-/-</sup> mice, strongly indicating an on-target effect of emixustat inhibition of visual cycle as well as scavenging atRAL. Previous studies in rats revealed that inhibition of VEGF using bevacizumab (avastin) antibody was able to prevent IR induced retinal permeability.<sup>21,25</sup> Similar studies in mice have yet to be reported, but it is likely that VEGF or inflammatory cytokines contribute to the IR-induced vascular permeability response in mice and account for the portion of the response not attributable to atRAL toxicity.

That atRAL per se contributes to vascular permeability was supported by multiple lines of evidence. First, we demonstrate that the permeability marker sulfo-NHS biotin was deposited in the basement membrane around the vascular bed of the inner retina after IR. Although

control group by 2-way ANOVA and post hoc test. (B) AtRAL induces solute permeability in BREC monolayers. BREC cells were grown to confluence on transwell filters and switched to stepdown media 48 hours before the addition of atRAL at the final concentrations indicated. Cell permeability to 70 kDa RITC-dextran was measured over a 3.5-hour time course starting at 2.5 hours after addition of atRAL. Data ( $n \geq 8$ /group) represent the relative diffusive permeability (Po) compared to the sham group, with all control values ranging between 0.4 and 0.7 × 10<sup>-6</sup> cm/sec. (C) Emixustat is able to block atRAL-induced permeability. BREC cells were plated on transwell filters and switched to stepdown media 48 hours before the addition of atRAL and/or emixustat. Cell monolayer permeability to 70 kDa RITC-dextran was measured 2.5 hours later with  $n \geq 7$ /group.

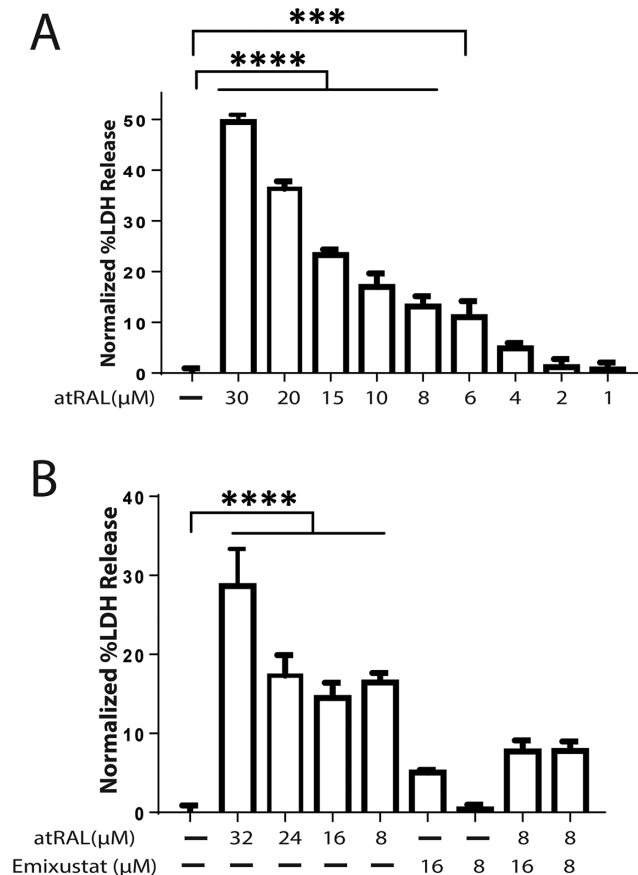


**FIGURE 6.** The atRAL induces cell death in endothelial cells. (A) BRECs were plated on 96-well culture plates and switched to step-down media 48 hours before the addition of atRAL for 4 hours at the indicated concentrations ( $n \geq 6$ /group). Cell viability was assessed by measuring the activity of LDH released into the media. Values were normalized to the total LDH activity released by cell lysis and subtracted from the percent of LDH released in the control group with no atRAL. (B) Emixustat is able to attenuate cell death induced by atRAL treatment. BRECs were plated on 96-well plates and cells were switched to step-down media 48 hours before the addition of atRAL and/or emixustat at the indicated concentrations ( $n \geq 6$ /group) and cell viability assayed by normalized LDH release in the media.

extensive staining could be observed around the normally permeable choroidal vessels, little or no leak was observed across the RPE. Second, atRAL acted directly on endothelial cells in culture to increase monolayer permeability to both ion flux and to 70 kDa RITC-dextran flux. The concentration response curve suggests that induction of endothelial cell damage or death directly contributed to increased endothelial permeability. Emixustat co-treatment with atRAL prevented the effects of atRAL on permeability and cell death, most likely through its documented ability to act as an atRAL scavenger. These studies also help to explain why MB-002, which can effectively inhibit RPE65 activity but lacks a primary amine group to scavenge atRAL, failed to inhibit IR-induced permeability. Both visual cycle inhibition and atRAL scavenging ability were necessary for the drug effectiveness of emixustat in vivo after IR. Similarly, emixustat was an effective inhibitor of light-induced damage to outer retina in *Abca4*<sup>-/-</sup>; *Rdh8*<sup>-/-</sup> mice, whereas MB-002 was ineffective.<sup>19</sup> It should be noted that *Abca4*<sup>-/-</sup>; *Rdh8*<sup>-/-</sup> mice were used in

the previous study because they exhibit increased accumulation of atRAL compared to normal mice upon light-induced damage. In the IR injury model, normal levels of atRAL seem to be sufficient to contribute to endothelial damage.

Using magnetic resonance imaging, a previous study observed accumulation of tracer in both the vascularized and avascular portions of the rabbit retina after IR, leading to the conclusion that leakage across the RPE occurred after injury.<sup>27</sup> Whereas, in the current study, cross-linkage of retina-accumulated NHS-biotin tracer allowed microscopic analysis at high resolution showing that nearly all vascular leakage was around the retinal blood vessels. These species differences may be due to the fundamental difference of retinal vessel anatomy, with the blood vessels confined to the medullary ray region that is superficial to the rabbit retina, rather than forming capillary networks in the ganglion, and inner nuclear region within the mouse retina. However, the present study does not preclude potential leak across the RPE at time points after IR injury that were not examined. However, the focus of this study was to determine if atRAL released from the photoreceptors can contribute to vascular permeability following retinal injury and if direct effects of atRAL on endothelial cells may cause this effect. Our data support these hypotheses.

Our in vitro studies suggest that atRAL can directly affect endothelial cells causing permeability and damage or death. Because the aldehyde group of atRAL is highly reactive, it is probably that the response is due to the direct effects of nucleophilic addition reactions with thiols and amines of cellular proteins. Several previous studies have documented cellular toxicity of atRAL.<sup>11–16</sup> Toxic effects of atRAL include membrane and DNA damage.<sup>28</sup> However, no studies have identified the precise molecular mechanism of atRAL toxicity. Interestingly, a recent study suggested that systemic retinaldehyde treatment can reduce visual dysfunction and retinal superoxide production in diabetes.<sup>29</sup> However, the systemic effect of the retinaldehydes may be very different than the local endothelial effect with systemic delivery potentially providing an anti-oxidant response or even conversion to active retinoic acid that acts through nuclear receptors. In the current study, the genetic, dark adaptation and chemical inhibition of the visual cycle provides compelling evidence that local atRAL contributes to vascular permeability in the retinal IR injury model.

The current results are consistent with a recent study of IRBP3 as a factor elevated in patients resistant to DR and acting as a potential protective factor.<sup>8</sup> IRBP3 was found to act in two mechanisms that may contribute to reduction in pathology of diabetic retinopathy. IRBP3 reduced VEGF signaling to endothelial cells and IRBP3 reduced GLUT1-mediated glucose uptake in Muller cells.<sup>8</sup> However, IRBP1 has been shown to reduce NADPH oxidase production of reactive oxygen species, mitochondrial dysfunction and cell death caused by atRAL treatment of 661W cell.<sup>30</sup> In addition, IRBP1<sup>-/-</sup> explant retinas had elevated atRAL after light exposure.<sup>30</sup> Therefore, the IRBP proteins may also act by binding and reducing free atRAL acting on vascular permeability.

In conclusion, in the IR model of retinal induced vascular permeability in mice, atRAL generated from the outer retina contributes to approximately half of the vascular permeability at the 48 hour time point. Recent studies suggest diabetes includes outer retina damage and, previous studies using the more limited visual cycle inhibitor retinylamine, already demonstrated efficacy in reducing retinal vessel loss and



capillary permeability in a diabetes model.<sup>17</sup> Herein, both in vitro and in vivo studies reveal that atRAL can act directly on capillary endothelial cells to induce permeability and cell death and suggest atRAL as a potential therapeutic target to control capillary permeability in retinal ischemic diseases.

### Acknowledgments

Supported by the National Institutes of Health (NIH) R24EY024864 (TSK), NIH R01EY029349 (SFA and DAA) and NIH EY012021 (DAA). The work was also supported by equipment and technical assistance provided by the Kellogg Eye Center Core Center for Vision Research, NIH P30EY007003 (Bret Hughes, PhD, Principal Investigator) and the Michigan Diabetes Research Center NIH P30-DK-020572.

Disclosure: **A. Dreffs**, None; **C.-M. Lin**, None; **X. Liu**, None; **S. Shanmugam**, None; **S.F. Abcouwer**, None; **T.S. Kern**, None; **D.A. Antonetti**, None

### References

- Arden GB. The absence of diabetic retinopathy in patients with retinitis pigmentosa: implications for pathophysiology and possible treatment. *Br J Ophthalmol*. 2001;85:366–370.
- Sternberg P, Jr, Landers MB, 3rd, Wolbarsht M. The negative coincidence of retinitis pigmentosa and proliferative diabetic retinopathy. *Am J Ophthalmol*. 1984;97:788–789.
- Kern TS, Berkowitz BA. Photoreceptors in diabetic retinopathy. *J Diabetes Investig*. 2015;6:371–380.
- Du Y, Veenstra A, Palczewski K, Kern TS. Photoreceptor cells are major contributors to diabetes-induced oxidative stress and local inflammation in the retina. *Proc Natl Acad Sci U S A*. 2013;110:16586–16591.
- Jain A, Saxena S, Khanna VK, Shukla RK, Meyer CH. Status of serum VEGF and ICAM-1 and its association with external limiting membrane and inner segment-outer segment junction disruption in type 2 diabetes mellitus. *Mol Vis*. 2013;19:1760–1768.
- Maheshwary AS, Oster SF, Yuson RM, Cheng L, Mojana F, Freeman WR. The association between percent disruption of the photoreceptor inner segment-outer segment junction and visual acuity in diabetic macular edema. *Am J Ophthalmol*. 2010;150:63–67 e61.
- Muftuoglu IK, Mendoza N, Gaber R, Alam M, You Q, Freeman WR. Integrity of outer retinal layers after resolution of central involved diabetic macular edema. *Retina*. 2017;37:2015–2024.
- Yokomizo H, Maeda Y, Park K, et al. Retinol binding protein 3 is increased in the retina of patients with diabetes resistant to diabetic retinopathy. *Sci Transl Med*. 2019;11:eaau6627.
- Kiser PD, Golczak M, Palczewski K. Chemistry of the retinoid (visual) cycle. *Chem Rev*. 2014;114:194–232.
- Kiser PD, Zhang J, Badiie M, et al. Rational tuning of visual cycle modulator pharmacodynamics. *J Pharmacol Exp Ther*. 2017;362:131–145.
- Chen Y, Okano K, Maeda T, et al. Mechanism of all-trans-retinal toxicity with implications for Stargardt disease and age-related macular degeneration. *J Biol Chem*. 2012;287:5059–5069.
- Zhu X, Wang K, Zhang K, Zhou F, Zhu L. Induction of oxidative and nitrosative stresses in human retinal pigment epithelial cells by all-trans-retinal. *Exp Cell Res*. 2016;348:87–94.
- Li J, Cai X, Xia Q, et al. Involvement of endoplasmic reticulum stress in all-trans-retinal-induced retinal pigment epithelium degeneration. *Toxicol Sci*. 2015;143:196–208.
- Getter T, Suh S, Hoang T, et al. The selective estrogen receptor modulator raloxifene mitigates the effect of all-trans-retinal toxicity in photoreceptor degeneration. *J Biol Chem*. 2019;294:9461–9475.
- Sawada O, Perusek L, Kohno H, et al. All-trans-retinal induces Bax activation via DNA damage to mediate retinal cell apoptosis. *Exp Eye Res*. 2014;123:27–36.
- Liao Y, Zhang H, He D, et al. Retinal pigment epithelium cell death is associated with NLRP3 inflammasome activation by all-trans retinal. *Invest Ophthalmol Vis Sci*. 2019;60:3034–3045.
- Liu H, Tang J, Du Y, et al. Retinylamine benefits early diabetic retinopathy in mice. *J Biol Chem*. 2015;290:21568–21579.
- Kubota R, Boman NL, David R, Mallikaarjun S, Patil S, Birch D. Safety and effect on rod function of ACU-4429, a novel small-molecule visual cycle modulator. *Retina*. 2012;32:183–188.
- Zhang J, Kiser PD, Badiie M, et al. Molecular pharmacodynamics of emixustat in protection against retinal degeneration. *J Clin Invest*. 2015;125:2781–2794.
- Lin CM, Titchenell PM, Keil JM, et al. Inhibition of atypical protein kinase C reduces inflammation-induced retinal vascular permeability. *Am J Pathol*. 2018;188:2392–2405.
- Abcouwer SF, Lin CM, Wolpert EB, et al. Effects of ischemic preconditioning and bevacizumab on apoptosis and vascular permeability following retinal ischemia-reperfusion injury. *Invest Ophthalmol Vis Sci*. 2010;51:5920–5933.
- Antonetti DA, Wolpert EB. Isolation and characterization of retinal endothelial cells. In Nag S, (Ed.), *The Blood-Brain Barrier: Biology and Research Protocols*. Totowa: Humana Press Inc., 2003:365–374.
- Harhaj NS, Felinski EA, Wolpert EB, Sundstrom JM, Gardner TW, Antonetti DA. VEGF activation of protein kinase C stimulates occludin phosphorylation and contributes to endothelial permeability. *Invest Ophthalmol Vis Sci*. 2006;47:5106–5115.
- Abcouwer SF, Lin CM, Shanmugam S, Muthusamy A, Barber AJ, Antonetti DA. Minocycline prevents retinal inflammation and vascular permeability following ischemia-reperfusion injury. *J Neuroinflammation*. 2013;10:149.
- Muthusamy A, Lin CM, Shanmugam S, Lindner HM, Abcouwer SF, Antonetti DA. Ischemia-reperfusion injury induces occludin phosphorylation/ubiquitination and retinal vascular permeability in a VEGFR-2-dependent manner. *J Cereb Blood Flow Metab*. 2014;34:522–531.
- Kurth I, Thompson DA, Ruther K, et al. Targeted disruption of the murine retinal dehydrogenase gene *Rdh12* does not limit visual cycle function. *Mol Cell Biol*. 2007;27:1370–1379.
- Wilson CA, Berkowitz BA, Funatsu H, et al. Blood-retinal barrier breakdown following experimental retinal ischemia and reperfusion. *Exp Eye Res*. 1995;61:547–557.
- Zhao J, Liao Y, Chen J, et al. Aberrant buildup of all-trans-retinal dimer, a nonpyridinium bisretinoid lipofuscin fluorophore, contributes to the degeneration of the retinal pigment epithelium. *Invest Ophthalmol Vis Sci*. 2017;58:1063–1075.
- Berkowitz BA, Kern TS, Bissig D, et al. Systemic retinaldehyde treatment corrects retinal oxidative stress, rod dysfunction, and impaired visual performance in diabetic mice. *Invest Ophthalmol Vis Sci*. 2015;56:6294–6303.
- Lee M, Li S, Sato K, Jin M. Interphotoreceptor retinoid-binding protein mitigates cellular oxidative stress and mitochondrial dysfunction induced by all-trans-retinal. *Invest Ophthalmol Vis Sci*. 2016;57:1553–1562.